Impact dynamics of granular jets with non-circular cross-sections

Xiang Cheng,[1,2] Leonardo Gordillo,[2,3] Wendy W. Zhang,[2] Heinrich M. Jaeger,[2] and Sidney R. Nagel[2]

[1]*Department of Chemical Engineering and Materials Science, University of Minnesota, Minneapolis, MN 55455*
[2]*The James Franck Institute and Department of Physics, The University of Chicago, Chicago, Illinois 60637*
[3]*Laboratoire "Matière et Systèmes Complexes" (MSC), UMR 7057 CNRS, Université Paris 7 Diderot, 75205 Paris Cedex 13, France*

(Dated: July 26, 2013)

Using high-speed photography, we experimentally investigate impact dynamics of granular jets with non-circular cross-sections. We reveal the detailed dynamics of the impact process and uncover three different regimes. In the steady-state regime, we observe the formation of thin granular sheets with anisotropic shapes. We show that the degree of anisotropy increases with the aspect ratio of the jet's cross-section. Our results unambiguously illustrate the liquid-like behavior of granular materials during impact, and demonstrate a universal feature for physical systems where a collective hydrodynamic flow emerges from strongly interacting discrete particles.

PACS numbers: 45.70.Mg, 47.55.Ca

I. INTRODUCTION

When a liquid jet impacts on a solid surface, it shatters violently, spreads out rapidly and deforms into an elegant thin film [1]. Such an impressive phenomenon has attracted both lay people and scientists. In 1833, well before the invention of high-speed photography, the French physicist Savart conducted a classical "water-bell" experiment and illustrated with precise hand-drawn pictures the dynamics of a water jet hitting a small disc [2]. The ubiquitous fluid impact process, occurring in many natural and industrial circumstances, is determined by non-equilibrium momentum and energy transfer between the fluid and the solid surface, and depends on fluid properties such as inertia, surface tension and viscosity [3, 4].

The pattern of ejecta during impact has been used to reveal some of the special fluid properties in different materials. For example, it has been found that a jet of granular materials hitting a solid target can form a hollow cone or a thin sheet, with a shape quantitatively matching that of a liquid *without* surface tension [5–7]. As another more esoteric example, the coherent ejecta patterns observed at the Relativistic Heavy Ion Collider (RHIC) have been thought to indicate that the quark-gluon plasma formed during impact of relativistic ions is a nearly perfect (zero-shear-viscosity) liquid [8, 9]. In spite of 16 orders of magnitude difference in their energy scales, the two examples share one common feature: they both illustrate emergent hydrodynamic flows out of strongly interacting discrete particles. Thus, a granular jet impact has been studied in part as a macroscopic analog of the RHIC experiment [5, 10, 11]. One attempt has been to model such ejecta patterns as a fluid with a finite viscosity [12, 13]. Indeed, similar to the anisotropic ejecta pattern of the quark-gluon plasma, an asymmetric granular sheet was produced in a granular jet experiment when a rectangular granular jet impinged on a solid target [5].

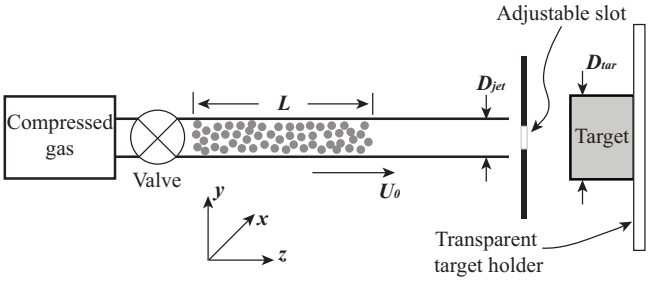

FIG. 1: A schematic of the experiment setup. The definition of the coordinate is also shown.

One outstanding feature of RHIC experiment is that the degree of anisotropy in the ejecta pattern varies with the impact parameter between two ions: while a head-on collision with zero impact parameter results in symmetric ejecta, a glancing collision with impact parameter close to the diameter of an ion leads to a highly anisotropic elliptic flow [9, 14]. Are the anisotropic ejecta patterns a universal feature of fluid impact? Can one mimic the variation of anisotropic ejecta in a classical fluid experiment? To answer these questions, the experimental challenge is to create a fluid jet with a non-circular cross-section of tunable aspect ratios. Such an asymmetric jet will induce a non-circular collision area upon impact, which simulates the collision zone of two partially overlapped relativistic ions [9, 14]. The experiment is difficult, if not impossible, to perform with normal liquids, where surface tension can cause strong oscillations in the shape of a non-cylindrical liquid jet and thus lead to an uncontrollable collision area. Here, we employ a granular material as a special fluid with negligible surface

tension [15, 16]. We perform a series of granular impact experiments using non-cylindrical granular jets with the aspect ratio of their cross-section ranging from 1 up to 6. We investigate the dynamics of granular jet impact and uncover three distinct regimes. Moreover, we show that the anisotropy of ejected granular sheet increases with the aspect ratio. Our results provide a new insight into the collective liquid-like behavior of granular materials and demonstrate a universal feature of the fluid-impact process. Beyond its academic interest as an analog to RHIC experiments, the results also show a new way to manipulate the impact dynamics of granular jets, which has been widely used in many industrial processes such as abrasive machining, sand-blast cleaning and polishing [17, 18].

II. EXPERIMENT

Our experiment setup is similar to that used in previous studies [5, 11]. It consists of a glass launching tube filled with a densely-packed granular material (Fig. 1). The tube has an inner diameter of $D_{Jet} = 1.5$ cm, and is connected to a high-pressure gas tank through a valve. The compressed gas in the tank can accelerate a granular column of length $L = 40$ cm to a speed $U_0 \sim 10$ m/s along the z direction before it hits a solid target placed 2.5 cm in front of the tube. The solid target has a diameter $D_{Tar} = 2D_{Jet}$ and is centered on the jet axis. To modify the cross-section of the jet, a small slot of prescribed shape and aspect ratio is inserted between the tube and the target. After passing through the slot, the jet acquires a cross-section with a shape approximately the same as the slot. Hence, by inserting different slots, we can control the shape of the jet's cross-section. A small gap of about 5 mm is left between the slot and the tube to avoid jamming of the moving jet inside the tube. A high-speed camera (Phantom v7) was used to image the impact dynamics at 2000 frames per second from behind the target along the negative z direction. To avoid optical obstruction, we construct a transparent target holder for some of our experiments. Throughout our experiment, we use mono-disperse glass beads of diameter 100 μm as our granular material. By tapping the launching tube, the beads are compacted into a density close to that of random-close packing before each experiment.

The azimuthal $(x - y)$ projection of the collision zone between two relativistic ions consists of two circular segments with an almond-like shape (Fig. 2A) [9, 14]. The aspect ratio of the zone, $c = y_1/x_1$, depends on the impact parameter, b, and the size of the ions. To manufacture slots of similar shape with controllable aspect ratio, we adopt the following machining protocol. First, holes of different sizes are drilled along a straight line (l_1) on two identical square polycarbonate plates (Fig. 2B),

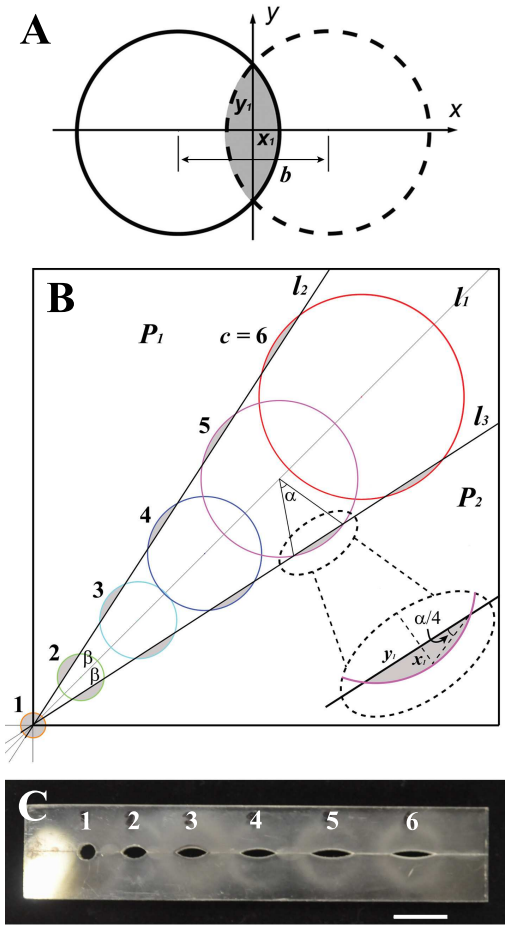

FIG. 2: (color online). Shape of granular jet's cross-section. (A) Collision zone between two relativistic heavy ions (gray area). The left ion (solid line) moves in the z direction out of the plane of the paper. The right ion (dashed line) moves in the negative z direction into the plane of the paper. x_1 and y_1 define the semi-axis of the collision zone. b is the impact parameter. (B) Schematic of the protocol for machining slots of different aspect ratios. The relation between α and c is shown in the lower right inset. (C) Slots of different aspect ratios. The scale bar is 15 mm.

where the radius of the i-th hole, R_i, and its center location along l_1, D_i, are determined by:

$$R_i = \left(\frac{\sigma}{\alpha_i - \sin\alpha_i}\right)^{1/2}, \tag{1}$$

and

$$D_i = \frac{R\cos(\alpha_i/2)}{\sin\beta}. \tag{2}$$

Here, $\alpha_i = 4\arctan(1/c_i)$, σ is the desired area of the slot, and β is an arbitrary angle that one chooses to cut the plates in the next step. Specifically, we drill six holes on each plate with $c_i = 1, 2, 3, 4, 5$ and 6 respectively and choose $\beta = 12°$. Unless noted otherwise, we fix $\sigma = 16.6$

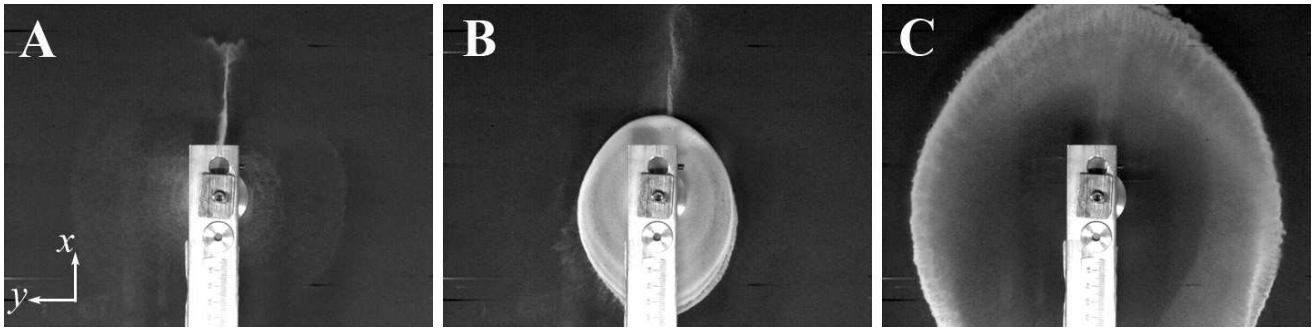

FIG. 3: Impact dynamics of granular jet with $\sigma = 26.6$ mm^2 and $c = 2$. (A) First regime; (B) Second regime; (C) Third regime. The long axis of the slot is along the y axis as indicated in (A). The target holder blocks the view of granular sheet partially. For example, in (A), the view of the stream shooting downward is blocked by the holder. The width of the holder is 3.0 cm.

mm^2. Next, we cut the first plate along line l_2 and cut the second plate along line l_3. Each of these two lines forms an angle $\beta = 12^\circ$ with respect to the central line l_1 (Fig. 2B). Joining part P_1 with part P_2 from these two cuts, we obtain six slots from the gray areas as indicated in Fig. 2B. The slots have the same area but varying aspect ratios from 1 to 6. The final slots are shown in Fig. 2C. Using these slots, we can generate granular jets with cross-sections that simulate the collision zone of relativistic heavy ions at different impact parameters.

III. RESULTS AND DISCUSSION

We fixed $D_{Tar} = 2D_{Jet}$ in our experiment. The ejected granular sheet is always perpendicular to the incoming jet. This is consisted with a previous study, where granular cones with apex angle $< 90^\circ$ sets in only when $D_{Tar}/D_{Jet} \leq 1.8$ [5]. In the rest of the paper, we only consider the shape of the ejected granular sheet in the $x - y$ plane.

The dynamics of granular jet impact shows three different regimes. We illustrate these regimes with a jet of $\sigma = 26.6$ mm^2 and $c = 2$ (Fig. 3A-C, and the Supplemental Material [19]). In the first regime, when the head of jet just impacts the target, the energy of the spreading ejecta is highly focused. The jet deforms into two thick streams, which shoot out in opposite directions along the short axis (the x axis) of the jet's cross-section (Fig. 3A). In the second regime, following the streams, an elliptical granular sheet emerges (Fig. 3B). The major axis of the elliptical sheet is along the short axis of the cross-section. The anisotropy of the elliptical sheet implies that particles that escape along the short axis of the collision zone have larger momentum. This anisotropic distribution of particle momentum demonstrates the liquid-like behavior of the granular jet. When a liquid state is formed inside the collision zone, a strong pressure gradient builds up along the short axis, which induces large particle momentum along that axis and leads to the observed elliptical flow pattern. As a comparison, if the granular jet shows a particle-like ideal gas behavior, the collisions between particles are uncorrelated. The distribution of particle momentum in the ejecta would be symmetric irrespective of the shape of collision zone. The same argument also applies to the RHIC experiment. Indeed, the asymmetric ejecta pattern has been used as a critical evidence for the liquid-like behavior of quark-gluon plasma [8, 9, 14]. Finally, towards the end of the impact, the density of particles fluctuates strongly. Small plugs of granular material interrupted by air gaps lead to concentric elliptical rings in this third regime (Fig. 3C).

The first regime of the impact is a transient state. As shown recently, during impact particles pile up in front of the target into a dead zone, where the mobility of the particles goes to zero [11]. The ejection of streams in the first regime may relate to the formation of the dead zone during initial impact. The granular jet reaches a steady state in the second regime. The energy of the ejecta is less focused, and the pattern is sustained over a longer time. Both the elliptical shape and the relative orientation of the ejecta are reminiscent of the anisotropic expansion pattern of strongly interacted Fermi gas atoms, where the interaction between individual atoms also leads to a collectively liquid-like behavior [20]. For a jet with smaller cross-section ($\sigma = 16.6$ mm^2), the transit regime is shorter and less pronounced (the Supplemental Material [19]).

In the steady-state second regime, the anisotropy of the ejecta also increases with time. The sheet is more isotropic when it first emerges. The degree of the anisotropy increases monotonically and reaches a maximum value towards the end of the second regime. To quantify the anisotropy, we follow the similar procedure used in RHIC experiment and previous granular jet study [5, 8]. The shape of the ejecta sheet is first extracted from the movie by choosing a proper threshold. If we assume that the granular sheets have uniform thickness during

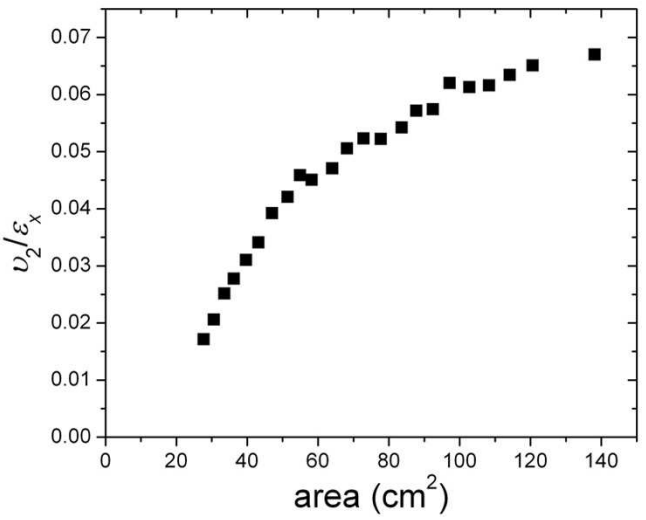

FIG. 4: Anisotropy of a granular sheet as a function of the area of the granular sheet in the second regime. The granular jet has an aspect ratio of $c = 4$.

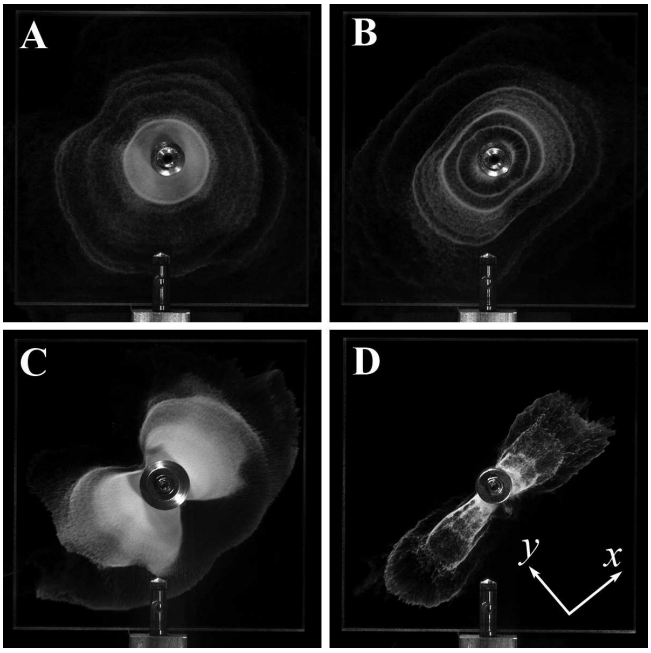

FIG. 5: Impact of granular jets with the aspect ratio of cross-section: (A) $c = 1$, (B) $c = 3$, (C) $c = 4$, and (D) $c = 6$. The slot orientation is shown by the coordinate in D.

each impact, the area of the ejecta is proportional to the number of ejected particles and increases with time. From the area at each azimuthal angle between θ and $\theta + \mathrm{d}\theta$, we can calculate the probability distribution of ejected particles, $P(\theta)$ along the direction as a function of time. $P(\theta)$ is normalized so that $\int_0^{2\pi} P(\theta)\mathrm{d}\theta$. The second coefficient, v_2, of the Fourier expansion of $P(\theta)$ can then be used to quantify the degree of anisotropy in the shape of ejected sheet. To compare with the RHIC result, we normalize v_2 by the geometric factor of the cross-section, $\varepsilon_x = (c^2 - 1)/(c^2 + 1)$. As a typical example, we show the evolution of v_2/ε_x in the second regime for a granular jet with $c = 4$ (Fig. 4). That figure shows that v_2/ε_x increases with the area of granular sheet, and slowly saturates to a maximum value towards the end of the second regime.

The maximal anisotropy depends on the aspect ratio of jet's cross-section. As expected, the jet with $c = 1$ shows a symmetric ejecta pattern (Fig. 5A). With $c = 1$, one cannot distinguish between particle-like and liquid-like behaviors. At $c = 3$, however, the pattern is less symmetric (Fig. 5B). It turns into a figure eight shape when $c = 4$ (Fig. 5C and the Supplemental Material [19]). At even higher $c = 6$, the shape of the ejecta is elongated into a long strip (Fig. 5D). Quantitatively, we plot $P(\theta)$ for different c in Fig. 6A. Due to gravity, the peak at $\theta = \pi/2$ is slight lower than that at $\theta = 3\pi/2$. Fig. 6B shows that the degree of anisotropy in the ejecta pattern increases with the aspect ratio. From $c = 2$ to $c = 6$, v_2/ε_x covers a large range from 0.02 to 0.18, which contains the range of RHIC result from 0.02 up to 0.09 [9] Different from our previous study, where the two strong streams in the transient state were chosen as the analog to RHIC results [5], we analyze the anisotropy of the granular sheet in the steady-state regime here. We find that v_2/ε_x is slightly smaller in this regime.

IV. CONCLUSIONS

We have illustrated the liquid-like behavior of granular materials by preforming granular impact experiments with non-cylindrical jets. The collective hydrodynamic behavior of granular jets is vividly demonstrated by the anisotropic shape of ejected granular sheet. Inspired by the RHIC experiments, we showed that the degree of anisotropy can be controlled by using jets of different aspect ratios. Our experimental technique for creating non-cylindrical granular jets can be easily extended to study the dynamics of granular jets of different cross-sections in other geometries [16, 21–23]. With the help of high-speed photography, we revealed a much richer impact dynamics than had been reported previously [5–7, 10–13]. Our experimental findings also pose new questions for future study. Can current simulation techniques be used to investigate such a highly non-equilibrium time-dependent process [10–13]? What is the relation between the initial transient state of granular impact and granular shock dynamics in loosely-compacted granular media [24–26]?

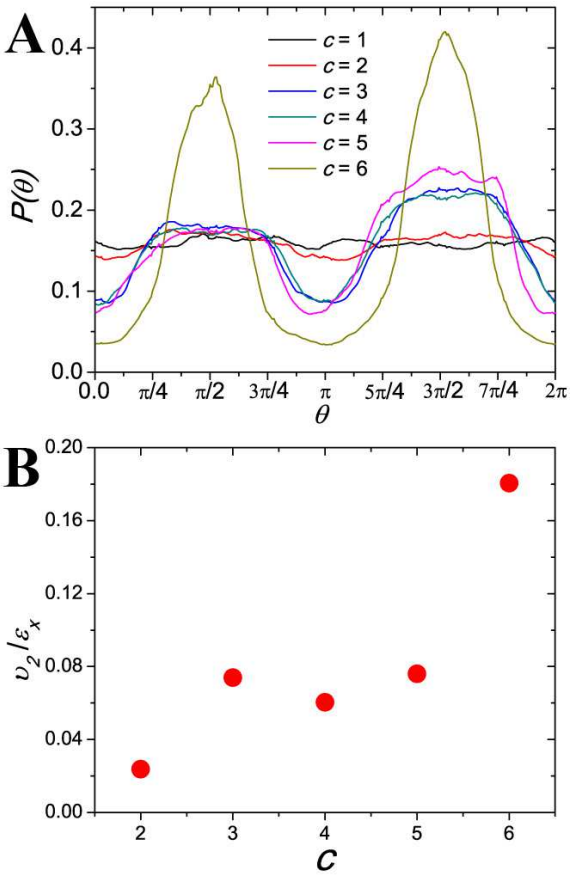

FIG. 6: (color online). Shape of granular sheets for jets of different cross-sections. (A) Probability distribution of ejected particles, $P(\theta)$, for different c. (B) Anisotropy, v_2/ε_x, as a function of c.

ACKNOWLEDGEMENTS

We are grateful to Ling-Nan Zou, Hervé Turlier and Daniel Citron, R. Bellwied and S. Gavin for helpful advice. This work was supported by the NSF MRSEC DMR-0820054. L.G. was supported by the NSF Materials World Network DMR-0807012.

[1] *A Gallery of Fluid Motion* edited by M. Samimy et al. (Cambridge University Press, Cambridge, UK, 2004).
[2] F. Savart, Ann. Chim. (Paris) **54**, 56 (1833); **54**, 113 (1833).
[3] C. Clanet, J. Fluid Mech. **430**, 111 (2001).
[4] C. Clanet, Annu. Rev. Fluid Mech. **39**, 469 (2007).
[5] X. Cheng, G. Varas, D Citron, H. M. Jaeger, and S. R. Nagel, Phys. Rev. Lett. **99**, 188001 (2007).
[6] Y. J. Huang, C. K. Chan, and P. Zamankhan, Phys. Rev. E **82**, 031307 (2010).
[7] N. Guttenberg, Phys. Rev. E **85**, 051303 (2012).
[8] I. Arsene et al. (BRAHMS Collaboration), Nucl. Phys. A **757**, 1 (2005); B. B. Back et al. (PHOBOS Collaboration), *ibid.* **757**, 28 (2005); J. Adams et al. (STAR Collaboration), *ibid.* **757**, 102 (2005); K. Adcox et al. (PHENIX Collaboration), *ibid.* **757**, 184 (2005).
[9] P. Braun-Munzinger and J. Satchel, Nature **448**, 302 (2007).
[10] J. Ellowitz, N. Guttenberg, and W. W. Zhang, arXiv:1201.5562 (2012).
[11] J. Ellowitz, H. Turlier, N. Guttenberg, W. W. Zhang, and S. R. Nagel, arXiv:1304.4671 (2013).
[12] T. G. Sano and H. Hayakawa, Phys. Rev. E **86**, 041308 (2012).
[13] T. G. Sano and H. Hayakawa, arXiv:1302.6734 (2013).
[14] T. Schafer and D. Teaney, Rep. Prog. Phys. **72**, 126001 (2009).
[15] X. Cheng, L. Xu, A. Patterson, H. M. Jaeger, and S. R. Nagel, Nature Phys. **4**, 234 (2008).
[16] J. Royer et al. Nature **459**, 1110 (2009).
[17] M. Seavey and J. Prot, Coatings and Linings **2**, 26 (1986).
[18] M. Achtsnicka, P. F. Geelhoedb, A. M. Hoogstratea, and B. Karpuschewski, Wear **259**, 84 (2005).
[19] See Supplemental Material for movies showing impact dynamics of non-cylindrical granular jets.
[20] K. M. O'Hara, S. L. Hemmer, M. E. Gehm, S. R. Granade, and J. E. Thomas, Science **298**, 2179 (2002).
[21] S. T. Thoroddsen and A. Q. Shen, Phys. Fluids **13**, 4 (2001).
[22] G. Caballero, R. Bergmann, D. van der Meer, A. Prosperetti, and D. Lohse, Phys. Rev. Lett. **99**, 018001 (2007).
[23] Y. Amarouchene, F. Boudet, and H. Kellay, Phys. Rev. Lett. **100**, 218001 (2008).
[24] Y. Amarouchene, F. Boudet, and H. Kellay, Phys. Rev. Lett. **86**, 4286 (2001).
[25] E. C. Rericha, C. Bizon, M. D. Shattuck, and H. L. Swinney, Phys. Rev. Lett. **88**, 014302 (2001).
[26] S. van den Wildenberg, R. van Loo, and M. van Hecke, arXiv:1304.6392 (2013).